Near-obstacle flight with small UAVs*

Jean-Christophe Zufferey, Antoine Beyeler, Dario Floreano

May 16, 2008

Abstract

Autonomous flight in confined or cluttered environments such as houses or urban canyons requires high manoeuvrability, fast mapping from sensors to actuators and very limited overall system weight. Although flying animals are well capable of solving this problem, roboticists have difficulties at reproducing such capabilities. This paper describes why and how we took inspiration from flying insects to progress toward the goal of developing small UAVs able to dynamically fly in cluttered environments. This endeavour allowed us to demonstrate a 10-gram microflyer capable of fully autonomous operation in an office-sized room using fly-inspired vision, inertial and airspeed sensors. This encouraging result is now being ported to outdoor scenarios such as low-altitude flight in urban or mountainous environments. Important is that these autonomous capabilities are achieved without the help of GPS or active range finders, which allows to develop very lightweight autopilots.

1 Introduction

Current UAVs tend to fly in open sky, far from any obstacles and rely on external beacons – mainly GPS – to localise themselves and navigate. This approach precludes them from evolving autonomously at low altitude, in cluttered or confined environments as insects do. At the Laboratory of Intelligent

*This work was supported by the Swiss National Science Foundation grant nr. 200020-116149.

Systems, we have been developing control strategies allowing for automating flight and collision avoidance without relying on external aids nor active distance sensors [32]. To achieve this, we took inspiration from flies and bees, studied their sensor suites and ways of processing information in order to extract principles that could then be applied to small artificial flyers. It turned out that insects are mainly relying on low-resolution, monocular vision [18], inertial [20] and airflow sensors [8]. This is interesting because the corresponding sensors are now available with small, light packaging, and extremely low power. Therefore, rather than opting for bulky active 3D range finders weighing a few kilograms [22], dynamic flight in the vicinity of obstacles can be achieved with far lower weight by using passive sensors such as vision, MEMS rate gyros and miniature anemometers.

Approximately two-thirds of the neurons in the insect brain are dedicated to visual information processing [28]. Biologists have unravel a significant part of their functioning. To make a long story short, image motion, also called *optic flow*, plays a significant role in flight control by providing information on self-motion [17, 15] and depth perception [26, 29, 9]. The good news for roboticists is that, as in insects, optic flow can be estimated with few pixels, allowing for the use of low-resolution vision sensors. The challenge is rather to have a large field of view (FOV) or at least cover divergent viewing directions, and grab images as fast as possible to obtain good approximations of optic flow.

Although quite recent, the idea of using optic flow for UAVs is not completely new and the first section of this paper is devoted to other research projects which obtained some noticeable result along this line. The second section presents the various steps it took us to achieve autonomous operation of a 10-gram microflyer inside a 7x6-m arena. Finally, we briefly comment about our current attempts at porting this result to faster, outdoor UAVs flying in cluttered environments.

2 Optic flow to steer UAVs

The optic flow is the perceived visual motion of surrounding objects projected onto the retina of an observer. The fact that visual perception of changes represents a rich source of information about self-motion and the depth of surrounding objects has been widely recognised for quite a long time [10]. If we assume a mobile observer moving in an otherwise stationary environment,

the motion field describing the projection of the object velocities onto its retina depends on its self-motion (translation and rotation), the distance to the surrounding objects, and the viewing directions [14]. In flying systems, it is usually feasible to estimate self-motion using a set of anemometers and rate gyroscopes. Optic flow can thus be used to estimate distance from surrounding objects.

Several teams have been looking at using this property of optic flow to estimate or control altitude of UAVs. Most of them were inspired by an experiment with honeybees describing how these insects execute grazing landing on horizontal surfaces [25, 27]. The first experiment of altitude control with a free-flying airplane was performed outdoors by Barrows and colleagues in 2002 with a 1-meter model airplane equipped with a custom-built optic-flow detector [2]. A simple (on/off) altitude control law managed to maintain the aircraft airborne for 15 minutes, during which 3 failures occurred where the human pilot had to rescue the aircraft due to it dropping too close to the ground. Further experiments were carried out on larger platforms for controlling descent rate [7], altitude above a flat and homogeneous surface [30], or to simply help with estimating altitude above ground [1]. All these experiments were focused on regulating altitude while the lateral steering was controlled by a safety pilot on ground.

The attempts at automating free-flying UAVs using bio-inspired vision are quite limited. In 2001, Barrows and colleagues described preliminary experiments on lateral obstacle avoidance in a gymnasium with a model glider carrying a single optic-flow sensor [3]. An accompanying video shows the glider steering away from a wall when tossed toward it at a shallow angle. More recently, a team in Washington carried out a second experiment on lateral obstacle avoidance with an indoor aircraft equipped with a single lateral optic-flow sensor [11]. A video shows the aircraft avoiding a basketball net in a sport hall. Since only one sensor was used, the aircraft could detect obstacles only on one side. In 2006, we used a 30-gram indoor airplane to demonstrate continuous and symmetrical collision avoidance in a relatively small arena of 16 by 16 m [33]. The robot was equipped with two miniature, custom-made, optic-flow detectors looking at 45° off the forward direction. A model proposed by Borst and Bahde [5] to account for landing response in flies was reused in this airplane to trigger saccadic turn-aways whenever a wall was too close. While altitude and airspeed was manually controlled, the airplane was able to fly collision-free for more than 4 min without any lateral

steering intervention from the human operator.[1] The plane was engaged in turning actions only 20% of the time, thus indicating that it was able to fly in straight trajectories except when very close to a wall. During a 4 min trial, it would typically generate 50 saccades, and cover approximately 300 m in straight motion.

On larger outdoor platforms, Griffiths and colleagues have used optic-flow mouse sensors as complementary distance sensors [12]. The UAV was fully equipped with an inertial measurement unit (IMU) and GPS. It computed the optimal 3D path based on a 3D map of the environment stored in its memory. In order to be able to react to unforeseen obstacles on the computed nominal path, it used a frontal laser range finder and two lateral optical mouse sensors. This robot demonstrated low altitude flight in a natural canyon while the mouse sensors provided a tendency towards the center when the nominal path was deliberately biased towards one or the other side of the canyon. Although no data showing the accuracy of measurements were provided, the experiment demonstrated that optical mouse sensors could be used to estimate rather large distances in outdoor environments. In 2005, Hrabar and colleagues [13] also employed lateral optic-flow to enable a large helicopter to center among obstacles outdoors, while stereo vision was utilized to avoid frontal obstacles. This work was quite similar to a study carried out in simulation by Muratet and colleagues the same year [19] and looking at optic-flow-based navigation in urban canyons. However, in these later projects the vision sensors were by no means used as primary sensors for navigation and the control system still relied mainly on traditional autopilot.

Although all these early attempts of mimicking insects and use optic flow to achieve flight control and collision avoidance are remarkable, it is to notice that none of them have reached the holy grail of completely automating a free-flying UAV without relying on additional information such as maps or GPS. The first project close to achieving this goal has been carried out in simulation by Neumann and Bülthoff [21]. A flying agent with a relatively simple helicopter-like dynamics could stabilise its course, control its altitude and avoid obstacles like trees using fly-inspired optic flow and matched filters [16, 31]. For their control strategy to work, the agent was required to be level at all the time. To ensure this, the attitude of the agent was constantly regulated using the intensity gradient, which was loosely inspired from the

[1] Video clips showing the behaviour of the plane can be downloaded from http://lis.epfl.ch/microflyers

insect ocelli [23]. However, for this attitude control mechanism to work, the environment needed to have a well-defined light intensity gradient, which is easy to ensure in simulated worlds, but not always available in real-world conditions.

Only very recently, we were able to get rid of any vertical reference and rely exclusively on optic flow in three specific directions (left, right and bottom) to achieve fully autonomous flight in a rectangular indoor environment [4]. Although the dynamics model of the airplane was quite realistic, this work was still only carried out in simulation. In the next section, we present what is, to the best of our knowledge, the first example of a fully autonomous physical airplane achieving optic-flow-based navigation in a confined environment. This endeavour was mainly driven by an attempt at finding the minimal set of sensors and control strategy that allows autonomous flight in 3D. Relying on the minimal number of pixels and optic-flow detectors was taken as a challenge that will eventually be loosened when porting the concept to other, potentially larger, platforms.

3 Autonomous flight indoors

As a first step towards the realisation of completely autonomous flying systems, we decided to impose dramatic weight constraints by developing an indoor flying platform. Flying indoor requires slow motion and small size, which calls for ultra-light overall weight. Our current prototype, the *MC2* (figure 1) is based on a remote-controlled 5.2-gram home flyer designed by Didel SA for the hobbyist market. This model consists mainly of carbon fiber rods and thin Mylar plastic films. The wing and the battery are connected to the frame by small magnets such that they can easily be taken apart. Propulsion is ensured by a 4-mm brushed DC motor, which transmits its torque to a lightweight carbon-fiber propeller via a 1:12 gearbox. The rudder and elevator are actuated by two magnet-in-a-coil actuators. The stock model airplane has been transformed into a robot by adding the required electronics and modifying the position of the propeller in order to free the field of view in the flight direction. When equipped with sensors and electronics, the total weight of the *MC2* reaches 10.3 g [34]. In its robotic configuration, the airplane is capable of flying in reasonably small spaces at low velocity (around 1.5 m/s). The average consumption is on the order of 1 W and the on-board 65 mAh lithium-polymer battery ensures an endurance of about 10

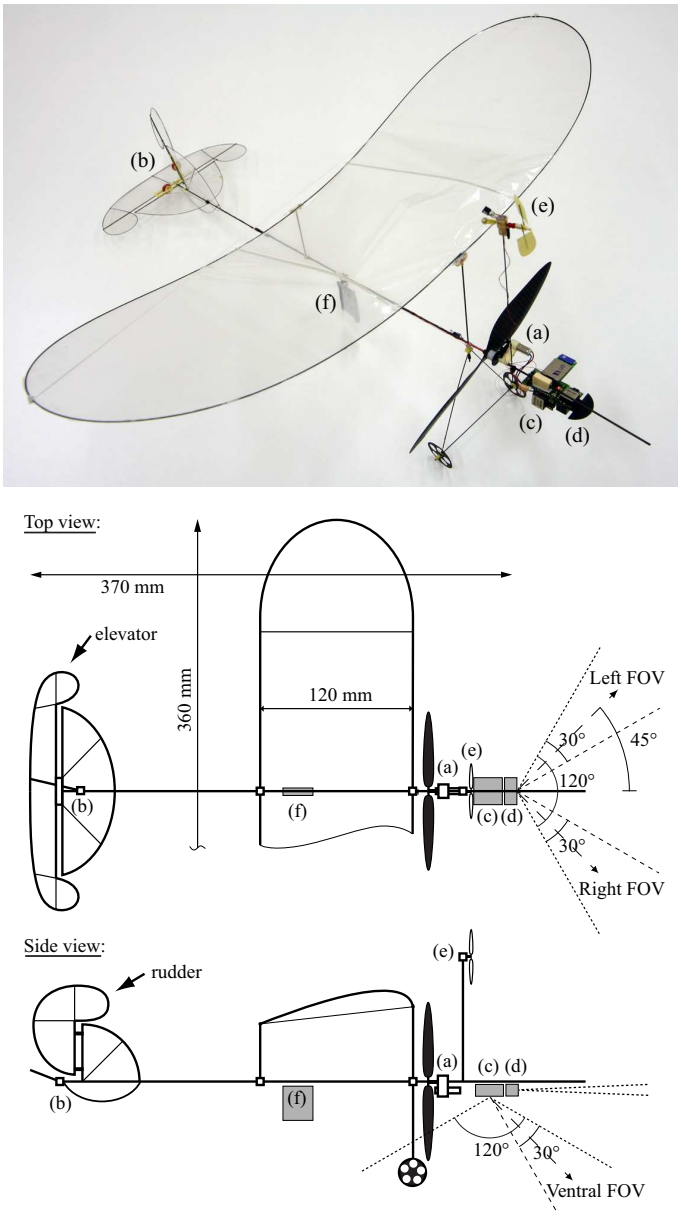

Figure 1: The 10-gram *MC2* microflyer. The on-board electronics consists of (a) a 4 mm geared motor with a lightweight carbon fiber propeller, (b) two magnet-in-a-coil actuators controlling the rudder and the elevator, (c) a microcontroller board with a Bluetooth module and a ventral camera with its pitch rate gyro, (d) a front camera with its yaw rate gyro, (e) an anemometer, and (f) a 65 mAh lithium-polymer battery.

minutes.

Regarding the sensor suite, we implemented the same sensory modalities as in flies. Since omnidirectional vision is not yet feasible within the available payload, we opted for two wide FOV, linear cameras. Only three segments of 20 pixels out of these two cameras have been selected for optic-flow extraction in three specific directions: left, right, and down. Additionally, two MEMS gyros have been mounted to sense pitching and yawing rates. Finally, a small custom-made anemometer ensures the functionality of airflow sensing. These sensors are connected to the onboard 8-bit microcontroller, which processes image sequences to estimate radial optic flow in the three viewing directions using an image interpolation algorithm [24, 33].

The rationale behind our control strategy is that optic flow estimates can be interpreted as proximity values if the following conditions are respected:

- the rotational optic-flow component (i.e. the optic flow due to self-rotations) is removed in order to keep only the translational part of it, which alone carries information about depth; this process is often referred to as *derotation*;
- the angle between the flight direction and the viewing direction of an optic-flow detector must be large enough to get usable optic-flow values; this is because the translational optic-flow amplitude is proportional to the sine of this angle [14, 32];
- the forward velocity of the airplane needs to be regulated in order to lower the impact of speed variations on optic flow.

The first condition is ensured by subtracting self-rotations as provided from the two rate gyros from the optic-flow measurements. This is possible because rotational optic flow is not sensitive to distances and we showed that its amplitude almost perfectly follows the rate gyro measurements when the airplane is undergoing pure rotational movements [33]. The second conditions is achieved by having an angle of 45° between the flight direction of the airplane (which is roughly parallel to the fuselage) and the viewing directions of the optic-flow detectors (OFD, see figure 2). The third condition is approximately met by means of a proportional controller linking the anemometer output to the torque applied to the main propeller. Optic-flow values can therefore be interpreted as proximity indicators, whose output can be mapped into actuator commands by means of simple weighted connections

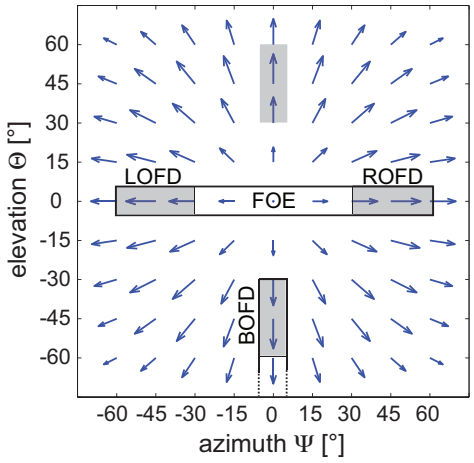

Figure 2: An azimuth-elevation graph displaying the zones (thick rectangles) covered by the two cameras mounted on the *MC2*. By carefully defining the sub-regions where optic-flow is extracted (gray zones within the thick rectangles), three radial optic-flow detectors (OFD) can be implemented at an equal eccentricity of 45° with respect to the flight direction. These are prefixed with L, B, and R for left, bottom and right, respectively.

(figure 3). This way of directly connecting inputs to outputs is inspired from Braitenberg [6] and allows for very reactive flight while avoiding computationally expensive deliberative layers.

The first tests of this control strategy were carried out in the same simulator as in [4], using a realistic model of the actual test room (figure 4). After some tuning of the parameters included in the Ω transfer functions (threshold and gains), the simulated *MC2* could efficiently circle the room (figure 5) while avoiding collisions with the ground and the surrounding walls. Once the controller was transferred to the physical airplane, the same behaviour occurred (a video can bee downloaded from http://lis.epfl.ch/microflyers). After being launched by hand in the test arena, the *MC2* would fly autonomously for a few minutes until caught by the experimenter.

Figure 6 shows data recorded during such an autonomous flight over a 90-s period. In the first row, the higher *RDOFD* signal (see figure 3 for an explanation of the variables) suggests that the airplane was launched closer to a wall on its right, which produced a leftward reaction (indicated by the negative yaw gyro signal) that was maintained throughout the trial duration.

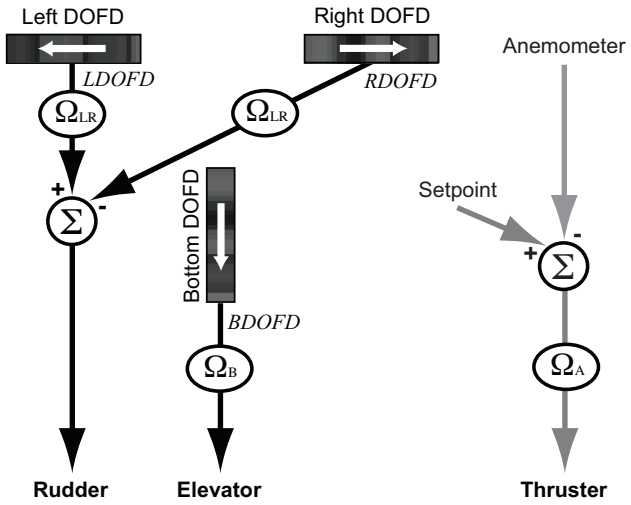

Figure 3: The control scheme for completely autonomous navigation and 3D collision avoidance. The three OFDs are prefixed with D to indicate that they are derotated. The signals produced by the left and right DOFDs, i.e. *LDOFD* and *RDOFD*, are basically subtracted to control the rudder, whereas the signal from the bottom DOFD, i.e. *BDOFD*, directly drives the elevator. The anemometer is compared to a given set-point to output a signal that is used to proportionally drive the thruster. The Ω ellipses indicate that a transfer function is used to tune the resulting behaviour. These can be simple gains or combinations of a threshold and a gain.

Note that in this environment, there is no good reason for modifying the initial turning direction since flying in circles close to the walls is more efficient than, for instance, describing eights. However, this first graph clearly shows that the controller does not simply hold a constant turning rate. Rather, the rudder deflection is continuously adapted based on the DOFD signals, which leads to a continuously varying yaw rotation rate. The average turning rate of approximately $80^\circ/\mathrm{s}$ indicates that a full rotation is accomplished every 4-5 s. Therefore, a 90 s trial corresponds to approximately 20 circumnavigations of the test arena. The second graph shows that the elevator actively reacts to the *BDOFD* signal, thus continuously affecting the pitch rate. The non-null mean of the pitch gyro signal is due to the fact that the airplane is banked during turns. Therefore the pitch rate gyro also measures a component of the overall circling behaviour. It is interesting to realise that the

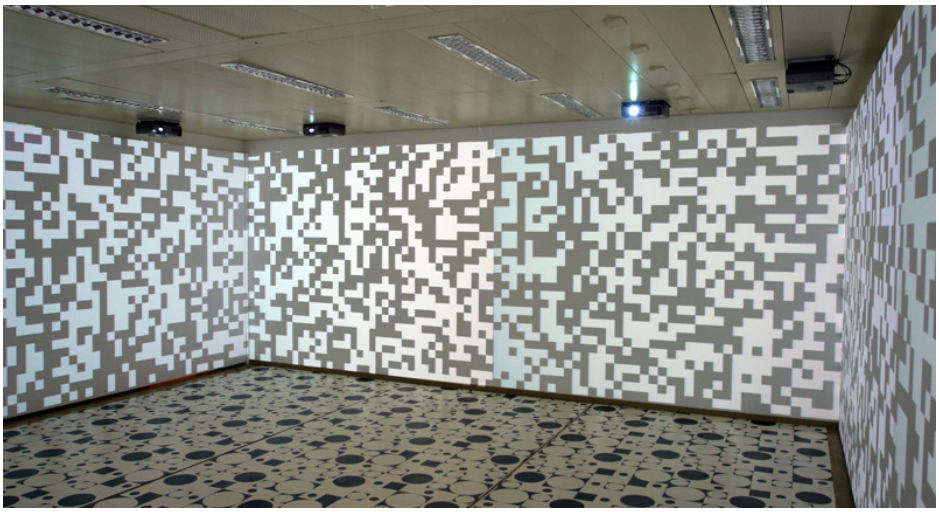

Figure 4: The 7 by 6 m test room for the *MC2* has 8 projectors attached to the ceiling, each projecting on half a wall. This system permitted an easy modification of the textures on the walls. The ground is covered by a randomly textured carpet.

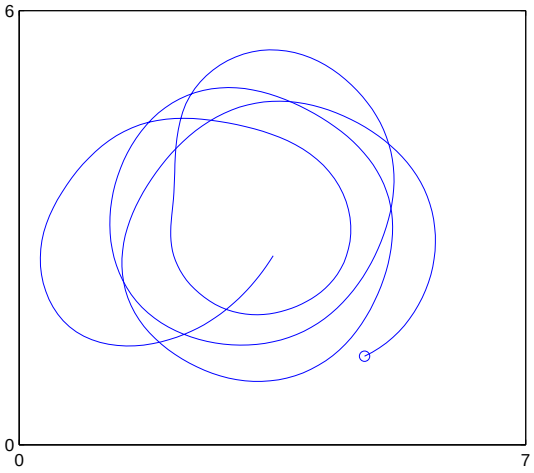

Figure 5: A top-view of a typical trajectory of the *MC2* in the 7x6-meter test arena. This trajectory has been obtained in simulation. However, as can be seen on the video at http://lis.epfl.ch/microflyers, the physical prototype displays a very similar behaviour.

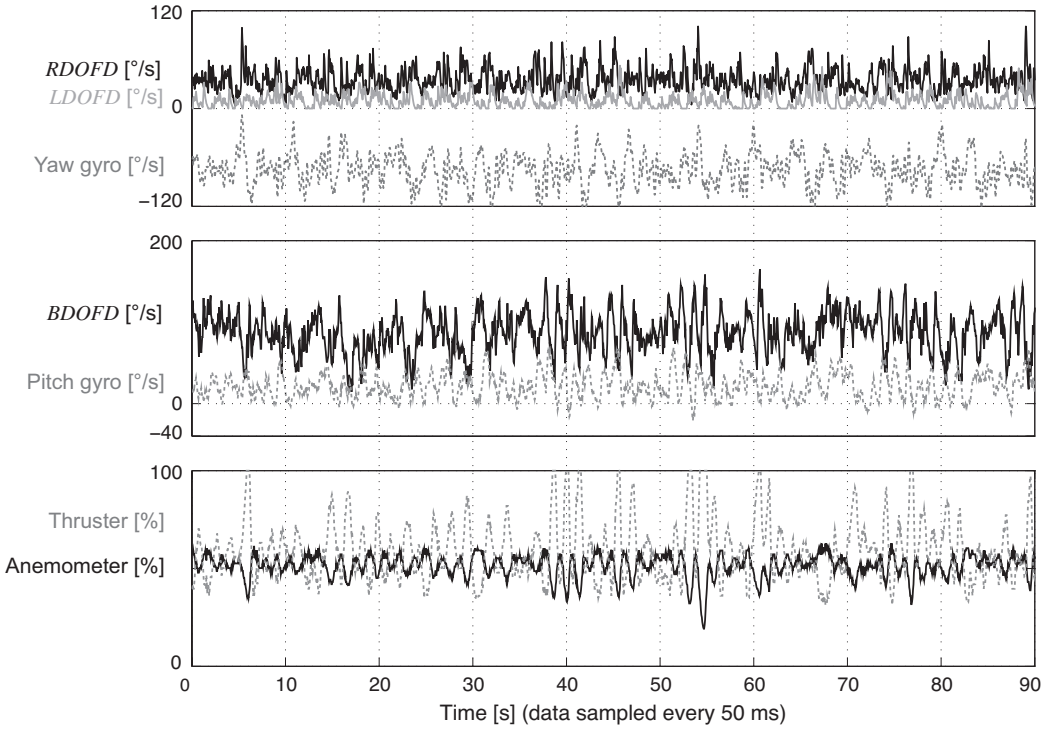

Figure 6: A 90-s autonomous flight with the *MC2*. The first row shows lateral OF signals together with the yaw rate gyro. The second row plots the ventral OF signal together with the pitch gate gyro. The third graph displays the evolution of the anemometer value together with the motor setting. Flight data are sampled every 50 ms, corresponding to the sensory-motor cycle duration.

elevator actions are not only due to the proximity of the ground, but also of the walls. Indeed, when the airplane feels the nearness of a wall to its right by means of its *RDOFD*, the rudder action increases its leftward bank angle. In this case the bottom DOFD is oriented directly towards the close-by wall and no longer towards the ground. In most cases, this would result in a quick increase in *BDOFD* and thus trigger a pulling action of the elevator. This reaction is highly desirable since the absence of a pulling action at high bank angle would result in an immediate loss of altitude. The bottom graph shows that the motor power is continuously adapted according to the anemometer value. In fact, as soon as the controller steers up due to a high ventral optic

Figure 7: The 300-gram flying wing testbed that will be used for optic-flow-based navigation in cluttered outdoor environments.

flow, the airspeed quickly drops, which needs to be counteracted by a prompt increase in thrust.

4 Conclusion and future work

Instead of flying straight and level between GPS way-points, flying in cluttered environments requires continuous maneuvering and quick reactions to avoid collisions. The use of insect-inspired sensors and control strategies allowed us to demonstrate autonomous operation of a 10-gram airplane in a confined environment. This is the result of a search for a minimal way of automating an ultralight flying system that cannot rely on classical sensors, nor external aids. We believe that the proposed control strategy[2] can easily be ported to larger platforms, which would allow for a greater number of pixels and thus more optic-flow detectors while keeping its reactive nature. Covering a larger fraction of the field of view will improve the robustness in presence of poorly textured or geometrically complex obstacles. Preliminary

[2]Patent pending: PCT/IB2008/051497

experiments in simulation demonstrated good results with a model of our 300-gram flying wing (figure 7) in various kinds of cluttered environments such as cities or hilly regions. We are now in the process of transferring these results to the actual UAV.

Since our control strategy is fast and simple, it has the potential, combined with higher-level control like goal-directed navigation, to bring near-obstacle flight missions into reality.

References

[1] D.B. Barber, S. Griffiths, T.W. McLain, and R.W. Beard. Autonomous landing of miniature aerial vehicles. In *AIAA Infotech@Aerospace*, 2005.

[2] G.L. Barrows, J.S. Chahl, and M.V. Srinivasan. Biomimetic visual sensing and flight control. In *Bristol Conference on UAV Systems*, 2002.

[3] G.L. Barrows, C. Neely, and K.T. Miller. Optic flow sensors for MAV navigation. In Thomas J. Mueller, editor, *Fixed and Flapping Wing Aerodynamics for Micro Air Vehicle Applications*, volume 195 of *Progress in Astronautics and Aeronautics*, pages 557–574. AIAA, 2001.

[4] A. Beyeler, J.C. Zufferey, and D. Floreano. 3D vision-based navigation for indoor microflyers. In *IEEE International Conference on Robotics and Automation (ICRA'07)*, 2007.

[5] A. Borst and S. Bahde. Spatio-temporal integration of motion. *Naturwissenschaften*, 75:265–267, 1988.

[6] V. Braitenberg. *Vehicles - Experiments In Synthetic Psychology*. The MIT Press, Cambridge, MA, 1984.

[7] J.S. Chahl, M.V. Srinivasan, and H. Zhang. Landing strategies in honeybees and applications to uninhabited airborne vehicles. *The International Journal of Robotics Research*, 23(2):101–110, 2004.

[8] R.F. Chapman. *The Insects: Structure and Function*. Cambridge University Press, 4th edition, 1998.

[9] M. Egelhaaf, R. Kern, H.G. Krapp, J. Kretzberg, R. Kurtz, and A.K. Warzechna. Neural encoding of behaviourally relevant visual-motion information in the fly. *Trends in Neurosciences*, 25(2):96–102, 2002.

[10] J.J. Gibson. *The Perception of the Visual World*. Houghton Mifflin, Boston, 1950.

[11] W.E. Green, P.Y. Oh, and G.L. Barrows. Flying insect inspired vision for autonomous aerial robot maneuvers in near-earth environments. In *Proceeding of the IEEE International Conference on Robotics and Automation*, volume 3, pages 2347– 2352, 2004.

[12] S. Griffiths, J. Saunders, A. Curtis, T. McLain, and R. Beard. *Obstacle and Terrain Avoidance for Miniature Aerial Vehicles*, volume 33 of *Intelligent Systems, Control and Automation: Science and Engineering*, chapter I.7, pages 213–244. Springer, 2007.

[13] S. Hrabar, G. S. Sukhatme, P. Corke, K. Usher, and J. Roberts. Combined optic-flow and stereo-based navigation of urban canyons for uav. In *IEEE International Conference on Intelligent Robots and Systems*, pages 3309–3316. IEEE, 2005.

[14] J.J. Koenderink and A.J. van Doorn. Facts on optic flow. *Biological Cybernetics*, 56:247–254, 1987.

[15] H.G. Krapp. Neuronal matched filters for optic flow processing in flying insects. In M. Lappe, editor, *Neuronal Processing of Optic Flow*, pages 93–120. San Diego: Accademic Press, 2000.

[16] H.G. Krapp, B. Hengstenberg, and R. Hengstenberg. Dendritic structure and receptive-field organization of optic flow processing interneurons in the fly. *Journal of Neurophysiology*, 79:1902–1917, 1998.

[17] H.G. Krapp and R. Hengstenberg. Estimation of self-motion by optic flow processing in single visual interneurons. *Nature*, 384:463–466, 1996.

[18] M.F. Land. Visual acuity in insects. *Annual Review of Entomology*, 42:147–177, 1997.

[19] L. Muratet, S. Doncieux, Y. Brière, and J.A. Meyer. A contribution to vision-based autonomous helicopter flight in urban environments. *Robotics and Autonomous Systems*, 50(4):195–209, 2005.

[20] G. Nalbach. The halteres of the blowfly calliphora. I. Kinematics and dynamics. *Journal of Comparative Physiology A*, 173(3):293–300, 1993.

[21] T.R. Neumann and H.H. Bülthoff. Behavior-oriented vision for biomimetic flight control. In *Proceedings of the EPSRC/BBSRC International Workshop on Biologically Inspired Robotics*, pages 196–203, 2002.

[22] S. Scherer, S. Singh, L. Chamberlain, and S. Saripalli. Flying fast and low among obstacles. In *Proceedings of the 2007 IEEE Conference on Robotics and Automation*, pages 2023–2029, 2007.

[23] H. Schuppe and R. Hengstenberg. Optical properties of the ocelli of calliphora erythrocephala and their role in the dorsal light response. *Journal of Comparative Physiology A*, 173:143–149, 1993.

[24] M.V. Srinivasan. An image-interpolation technique for the computation of optic flow and egomotion. *Biological Cybernetics*, 71:401–416, 1994.

[25] M.V. Srinivasan, J.S. Chahl, M.G. Nagle, and S.W. Zhang. Embodying natural vision into machines. In M.V. Srinivasan and S. Venkatesh, editors, *From Living Eyes to Seeing Machines*, pages 249–265. 1997.

[26] M.V. Srinivasan, M. Lehrer, W.H. Kirchner, and S.W. Zhang. Range perception through apparent image speed in freely-flying honeybees. *Visual Neuroscience*, 6:519–535, 1991.

[27] M.V. Srinivasan, S.W. Zhang, J.S. Chahl, E. Barth, and S. Venkatesh. How honeybees make grazing landings on flat surfaces. *Biological Cybernetics*, 83:171–183, 2000.

[28] N.J. Strausfeld. *Atlas of an Insect Brain.* Springer, 1976.

[29] L.F. Tammero and M.H. Dickinson. The influence of visual landscape on the free flight behavior of the fruit fly drosophila melanogaster. *The Journal of Experimental Biology*, 205:327–343, 2002.

[30] S. Thakoor, J.M. Morookian, J.S. Chahl, B. Hine, and S. Zornetzer. BEES: Exploring mars with bioinspired technologies. *Computer*, 37(9):38–47, 2004.

[31] R. Wehner. Matched filters - neural models of the external world. *Journal of Comparative Physiology A*, 161:511–531, 1987.

[32] J.-C. Zufferey. *Bio-inspired Flying Robots: Experimental Synthesis of Autonomous Indoor Flyers*. EPFL/CRC Press, 2008.

[33] J.-C. Zufferey and D. Floreano. Fly-inspired visual steering of an ultralight indoor aircraft. *IEEE Transactions on Robotics*, 22:137–146, 2006.

[34] J.-C. Zufferey, A. Klaptocz, A. Beyeler, J.-D. Nicoud, and D. Floreano. A 10-gram vision-based flying robot. *Advanced Robotics, Journal of the Robotics Society of Japan*, 21(14):1671–1684, 2007.